

# Comparison between $K$ and $\alpha$ sampling constants with the Pierre Gy's factors for bauxite

<http://dx.doi.org/10.1590/0370-44672022760033>

**Maria Teresa Marques<sup>1,2</sup>**

<https://orcid.org/0000-0003-0105-250X>

**Ana Carolina Chieregati<sup>1,3</sup>**

<https://orcid.org/0000-0002-6208-2924>

<sup>1</sup>Universidade de São Paulo – USP,

Departamento de Engenharia de Minas e Petróleo,  
São Paulo – São Paulo - Brasil.

E-mails: <sup>2</sup>[mariateresagcm@gmail.com](mailto:mariateresagcm@gmail.com),

<sup>3</sup>[ana.chieregati@usp.br](mailto:ana.chieregati@usp.br)

## Abstract

Sampling is an important tool for gathering information about mineral deposits, helping to estimate the ore grade, and has great relevance at any stage of a mining project, to ensure reliable results and consequently, to project a better mining planning. There are several errors to which the sampling is exposed and among them we can mention the fundamental sampling error (FSE). This error cannot become zero as it is related to the constitutional heterogeneity of the ore, so it represents the minimum sampling error. This study applies Pierre Gy's theory of sampling (TOS) to estimate the values of  $K$  and  $\alpha$  sampling constants at different deposits of bauxite in Brazil and compare them with the calculated factors, then calculate the relative standard deviation of the fundamental sampling error (FSE) based on the results of the heterogeneity test (HT) in each deposit. The deposits are located in: Barro Alto - State of Goiás, Juruti - State of Pará, and Poços de Caldas - State of Minas Gerais. The weathering process is the main reason of the alteration of the physical and chemical factors diversifying bauxites in Brazil and worldwide. However, when sampling is carried out correctly, the Gy's formula becomes a powerful tool for improving mining processes as long as the factors are estimated correctly for each ore.

**keywords:** Pierre Gy's theory of sampling, fundamental sampling error, heterogeneity test, bauxite.

## 1. Introduction

Aluminum ore, or simply bauxite, was discovered in 1821 by the Frenchman Pierre Berthier, who discovered it near the village of *Lês Baux*, in the south of France. It is a reddish land that contains high-grade aluminum ore, with about 40% alumina ( $Al_2O_3$ ) (Sampaio *et al.*, 2008). Currently, bauxite is the main raw material in the production of aluminum metal, being composed basically of gibbsite, diaspora and boehmite, which are considered aluminum oxyhydroxides (Arenare, 2008).

According to Monteiro and Silva (2018), the total of the world's bauxite reserves is around 27.9 billion tons, with Guinea and Australia being the largest holders. Brazil is ranked third, with approximately 2.7 billion tons. Among the states of the federation, Pará represents

89.5% of the national bauxite production, and has great potential for growth.

In the case of the evaluation of mineral deposits, or process control and marketing of the product, the importance of sampling is irrefutable (Luz *et al.*, 2004).

Sampling aims at the estimation of a quality parameter of a population, such as the grade. However, the mineral constituents of a deposit vary from point to point, making it unlikely that a single sample accurately represents the overall composition of the sampled unit (Arioli and Andriotti, 2007). It should be noted that bad sampling can result in considerable losses or distortions of results, with unpredictable technical and financial consequences. Sampling is one of the most complex operations and can easily introduce errors in the metallurgical and

mining industries (Luz *et al.*, 2004).

The current emphasis on understanding the natural variability of the deposit and source of sampling errors has arisen out of the theory of sampling (TOS) by Pierre Gy, who, in 1951, wrote an article entitled "Minimum mass of a sample needed to represent a mineral lot" (Minnitt *et al.*, 2007).

According to Gy (1998), the representativeness must be maintained at all stages of the sampling process. By ensuring the precision and accuracy of the samples taken at all stages of the mineral chain, the results will be auditable and reproducible.

Among the sampling errors that contribute to the non-representativity of the samples, Pitard (2005) listed ten: in situ nugget effect (NE); fundamental sampling error (FSE); grouping and seg-

regation error (GSE), long-range heterogeneity (Quality) fluctuation error (shifts and trends, QFE1), long-range periodic heterogeneity (Quality) fluctuation error (cycles, QFE2), incremental delimitation error (IDE), incremental extraction error (IEE), incremental weighing error (IWE), incremental preparation error (IPE), and analytical error (AE).

According to Gy (1982) the total sampling error (TSE) can be divided into separate components: random errors – which can be reduced, but never eliminated = NE + FSE + GSE + QFE1 + QFE2, and systematic errors – which can be eliminated when correct sampling procedures are performed = IDE+IEE+IWE+IPE+AE.

The fundamental sampling error is

$$s^2 (FSE) = c f g l d_N^3 \left( \frac{1}{M_s} - \frac{1}{M_L} \right) \quad (1)$$

where *c* is the mineralogical factor, *f* is the shape factor, *g* is the granulometric factor, and *l* is the liberation factor obtained using the liberation diameter *d<sub>l</sub>*, *d<sub>N</sub>* is the fragment nominal diameter or top size, *M<sub>s</sub>* is the sample mass, and *M<sub>L</sub>* is the

lot mass. As mentioned, these factors can be replaced by the constant *K*. However, due to the great difficulty in estimating these factors, HT is used, which allows the calculation through the calibration of the heterogeneity parameters *K* and *α*, where

one of the errors that cannot be eliminated because it is related to the constitutional heterogeneity of the ore, which has been pointed out as the source of all sampling errors (Gy, 1998). It is worth noting that the constitutional heterogeneity constant factor *IH<sub>L</sub>* can be calculated by obtaining several other factors, according to Gy's formula in Equation (1) (Minnitt *et al.*, 2007):

$K = c f g l$  and  $\alpha = \text{exponent of } d$ .

In summary, the objective of this study was to estimate the values of *K* and *α* sampling constants in different deposits of bauxite from Brazil, and to compare them with the calculated Gy's factors for each deposit.

## 2. Materials and methods

### 2.1 Bibliographic survey

First, a bibliographical survey was carried out to survey the mineral-

ogical characteristics of the ore from three bauxite deposits of different

geological formations, belonging to different companies.

### 2.2 Heterogeneity test (HT)

For the calibration of the *K* and *α* sampling constants, the methodology proposed by Pitard (2004) was applied for indirectly estimating the constitutional heterogeneity constant

factor (*IH<sub>L</sub>*).

Initially, the samples from deposits 1 and 2 were collected by the companies in different quantities so that they could be submitted to HT. Moreover, they were

crushed and arranged in an elongated pile (Fig. 1) for homogenization and primary quartering. The samples from deposit 3 were the same as those used in the article from Alves *et al.* (2020).

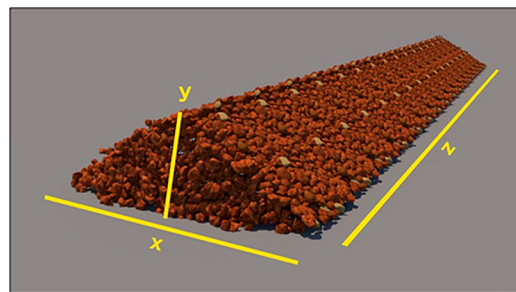


Figure 1 - Example of the elongated homogenization pile, where *x* represents width, *z* length and *y* height. Source: Drawn by the author using SketchUp Software.

The ideal mass to perform the test was collected from the pile, with this being variable from company to company. In sequence, the fraction collected was screened into four size fractions for the samples from Barro Alto and Juruti, and in three fractions for the sample from Poços de Caldas, resulting in the nominal top-size of the fragment (*d<sub>N</sub>*). It is worth mention-

ing, that the native bauxite from Poços de Caldas has a very fine granulometry when compared to the typical bauxite from other Brazilian states and, therefore, only three size fractions were used (Alves *et al.*, 2020).

According to Pitard (1993), the method consists in the extraction of a *Q* number of fragments, randomly collected from all size fractions of the investigated

material. In the case of ores with metal of interest in low concentration,  $Q \geq 100$  is used. For ores such as bauxite, with high concentration,  $Q \geq 50$  is used. It is suggested that the number (*N*) of fragments present in each particle size fraction be at least 10 times larger than the number of fragments (*Q*) multiplied by the number of groups collected (*p*), Equation (2):

$$N > 10 Q p \quad (2)$$

After confirming the total number of fragments per particle size fraction, an individual fragment was weighed, and the minimum sample mass was calculated to

compose each fraction. Each sample had to be homogenized and placed in a matrix with a square mesh (totalling 50 squares) (Fig. 2). Care should be taken to avoid over-

lapping fragments or even empty spaces; in other words, the fragments should be scattered so that every fragment has the same chance of selection.

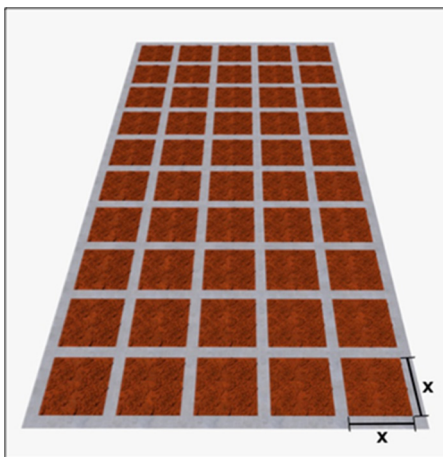


Figure 2 - Illustration of the square mesh for arrangement and collection of the fragments that make up the final sample whose dimension  $x$  is variable. Source: Drawn by the author using SketchUp Software.

In the next step, one fragment of each square was collected, composing a group, or sub-sample, comprising 50 fragments. The previous procedure was repeated 50 times, forming 50 groups of

at least 50 fragments per size fraction. The groups of fragments or sub-samples were then identified, weighed, separated, and placed in plastic bags. Each group was weighed to obtain the mass ( $M_g$ ) and sent

for chemical analysis for determination of the grade ( $a_g$ ) of usable alumina. All the data were tabulated and used for the construction of the graphs that will be discussed later.

### 3. Results and discussions

As mentioned in the previous section, a bibliographical survey was first

carried out for the characterization of the bauxite deposits of the three study sites:

Barro Alto, Juruti and Poços de Caldas known as deposits 1, 2 and 3, respectively.

#### 3.1 Deposit characterization

##### 3.1.1 Deposit 1, State of Goiás

The bauxite deposit located in the region of Barro Alto, state of Goiás, was discovered at the end of the 90s (Oliveira, 2011). Its genesis occurred on neoproterozoic anorthosites (Santos, 2011), located in the northern portion of the Mafic Ultramafic Complex of Barro Alto.

According to the climate classification of Köppen-Geiger (Kottek *et al.*, 2006), for being in a tropical climate, hot and rainy, the weather had a great impact on the anorthosite, generating deposits of bauxite with grades above

50% of usable  $Al_2O_3$  and a reserve estimated at 100 million tons. This deposit is unique, complex, and peculiar, with a profile of alteration represented by a bauxite saprolite located close to the important nickel laterite deposit of the same municipality (Santos, 2011).

Santos (2011) states that the profiles are highly evolved, constituting a body of ore that has five lithologies from top to bottom:

A. Colluvium bauxite: fragments of bauxite disaggregated from the pre-existing bauxitic facies.

B. Massive bauxite: formed from the remobilization of aluminum in a second phase of bauxitization, in which the microcrystalline texture of gibbsite fills the pores and fractures of primary bauxite.

C. Clay with bauxite blocks: constituting the portion in which a higher volume of kaolinite is associated with gibbsite.

D. Porous Bauxite: considered as isalterite with preserved structures of the anorthosite.

E. Anorthosite: bedrock.

##### 3.1.2 Deposit 2, State of Pará

This bauxite deposit is located in the sub-basin of the lower Amazon, Alter do Chão formation, in the town of Juruti, state of Pará (Carvalho, 1989). According to Patterson (1967) and Carvalho (1989), the Amazonian bauxite deposits are classified as "Blankets", formed "in situ" by processes of weathering on clastic sedimentary rocks in humid tropical climate conditions, Köppen-Geiger classification in Kottek *et al.* (2006). These deposits have thicknesses that vary up to 10 meters, presenting notable lateral

variations in the contents of aluminum, silica, and iron.

The typical lithological profile of the deposit 2, from top to bottom, is described as in Bortoleto *et al.* (2014):

A. Yellow clay (known as Belterra): consisting of a very uniform and permeable cover of kaolinitic yellow clay.

B. Nodular bauxite: composed of fine gibbsite nodules of varying sizes and distributed in a kaolinitic matrix.

C. Laterite: corresponding to a low silica horizon, presenting considerable variations in hardness, texture,

color, iron-aluminum ratio, and silica grade, which can be classified as ferruginous bauxite in some places.

D. Massive bauxite (bauxite layer): horizon composed of gibbsite, hematite, and kaolinite with economic value. The hardness, texture and color of the material varies according to the iron and clay content.

E. Variegated clay: consisting of a horizon composed of variegated kaolinitic clay, usually reddish to pink, with whitish spots and purple hues, possibly containing gibbsite.

### 3.1.3 Deposit 3, State of Minas Gerais

The alkaline plateau of Poços de Caldas has an area of approximately 800 km<sup>2</sup>, being located on the border between the states of São Paulo and Minas Gerais. The region is composed basically of phonolites and nepheline syenite, which makes this plateau one of the largest alkaline plateaus in the world (Ellert, 1959).

The bauxite deposits of this region are associated with alkaline intrusive rocks and are classified into two types: massive edge bauxite and plateau bauxite.

### 3.2 Heterogeneity test (HT)

In order to obtain the fundamental sampling error and the values of the *K* and *α* constants, the grades (*a<sub>q</sub>*) of available alumina and the masses (*M<sub>q</sub>*) resulting from the 50 samples obtained from each of the established size fractions were first determined. The size fractions used were (Silva, 2019):

ite. The bauxite formation in the area is reported as a direct and continuous process whose most important factors of influence are the topography, the nature of the bedrock, and the climatic conditions (Carvalho, 1989).

It is worth mentioning that the main mineral found in the region is gibbsite which is located mainly in the north of the plateau. In addition, the bauxite profiles can be classified as (Leonardi *et al.*, 2010):

- - 38.1 mm + 25.4 mm;
- - 25.4 mm + 12.7 mm;
- - 12.7 mm + 6.3 mm;
- - 6.3 mm + 1.2 mm.

The four size fractions were used for the bauxite samples of Barro Alto and Juruti (Bortoleto *et al.*, 2014) and the last three for the aluminum ore from Poços de

A. Reworked bauxite profiles: presence of bauxite gravel, similar to those found in mountain and plain profiles.

B. Bauxite profiles of mountain: located in the high altitudes of the plateau, they have a high concentration of aluminum, and are thick and well developed.

C. Bauxite plain profiles: located in the low altitudes of the plateau, they have small thickness, a low grade of aluminum, and are very clayey materials.

Caldas (Alves *et al.*, 2020).

After this, the value of the estimated *IH<sub>L</sub>* was calculated for each of the size fractions according to Equation (3) (Pitard, 1993). It is worth remembering that the value to be used for the granulometric factor (*g*) is 0.55 for calibrated materials (Chieregati and Pitard, 2018).

$$EST\ IH_L = g \sum \frac{(a_q - a_Q)^2}{a_Q^2} \frac{M_q^2}{M_Q} \quad (3)$$

where, *EST IH<sub>L</sub>* = estimated constitutional heterogeneity constant factor, *g* = granulometry factor, *a<sub>q</sub>* = individual

sample grade, *a<sub>Q</sub>* = average grade, *M<sub>q</sub>* = mass, and *M<sub>Q</sub>* = total mass.

To obtain the values of *M<sub>Q</sub>* and *a<sub>Q</sub>*,

$$M_Q = \sum M_q \quad (4)$$

$$a_Q = \frac{1}{M_Q} \sum a_q M_q \quad (5)$$

Then, it was necessary to obtain the nominal top size (*d<sub>N</sub>*) of the fragments in the different size fractions

to establish a correlation with the constant factor of heterogeneity, according to Equation (6) (Minnitt and

Assibey-Bonsu, 2010). The results are shown in Table 1.

$$d_N = \sqrt[3]{\frac{(d1^3 + d2^3)}{2}} \quad (6)$$

in which *d1* and *d2* represent the openings of the upper and lower sieves of each size fraction.

Table 1 - Heterogeneity factors correlated to each nominal topsize.

Deposit 1		Deposit 2		Deposit 3	
Nominal diameter ( <i>d<sub>N</sub></i> ) cm	<i>EST IH<sub>L</sub></i>	Nominal diameter ( <i>d<sub>N</sub></i> ) cm	<i>EST IH<sub>L</sub></i>	Nominal diameter ( <i>d<sub>N</sub></i> ) cm	<i>EST IH<sub>L</sub></i>
3.297	0.870	3.297	0.117	-	-
2.097	0.147	2.097	0.035	2.097	0.119
1.048	0.037	1.047	0.013	1.047	0.016
0.543	0.016	0.501	0.002	0.501	0.004

Subsequently, the *K* and *α* constants were estimated by plotting the

bi-log graph and power regression lines of the results in Table 1.

The trend line of the graph provides an equation that allows calibrat-

ing the  $K$  and  $\alpha$  sampling parameters for the different bauxite deposits,

replacing the Gy's factors according to Equation (7):

$$s^2(FSE) = K d_N^\alpha \left( \frac{1}{M_S} - \frac{1}{M_L} \right) \quad (7)$$

where  $s^2(FSE)$  represents the variance of the fundamental sampling error,  $K$  is the sampling constant for each ore type,  $d_N$

the nominal diameter,  $\alpha$  is the exponent of the original cubic formula of Pierre Gy, and  $M_S$  and  $M_L$  are, respectively, the

masses of the sample and of the lot. The bi-log correlations are shown in Fig. 3, Fig. 4, and Fig. 5.

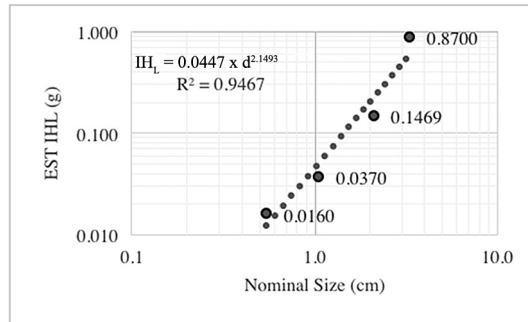


Figure 3 - Correlation between  $EST\ IH_L$  and  $d_N$  of the deposit 1.

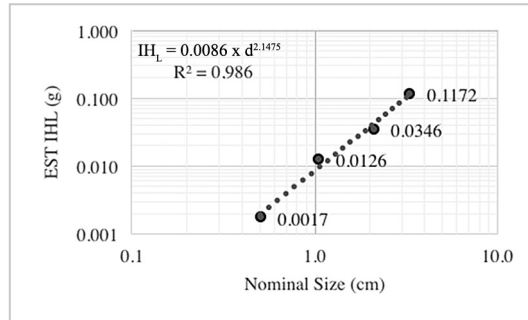


Figure 4 - Correlation between  $EST\ IH_L$  and  $d_N$  of the deposit 2.

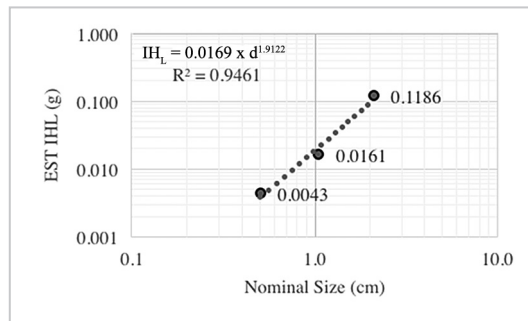


Figure 5 - Correlation between  $EST\ IH_L$  and  $d_N$  of the deposit 3.

The equation in the form " $y=c \cdot x^b$ ", observed in Figure 3, Figure 4, and

Figure 5, results in the sampling constants  $K$  ( $c$ ) and  $\alpha$  ( $b$ ), as shown in

Table 2, i.e., " $IH_L = Kd^\alpha$ ", according to Equation (7).

Table 2 - Estimated parameters  $K$  and  $\alpha$  for each bauxite mine in this study.

Deposit 1		Deposit 2		Deposit 3	
$K$	$\alpha$	$K$	$\alpha$	$K$	$\alpha$
0.0447	2.1493	0.0086	2.1475	0.0169	1.9122

After obtaining the sampling constants, the relative standard deviation of the fundamental sampling error  $s(FSE)$  can be determined. Pitard

(1993) suggests a maximum standard deviation of:

- $s(FSE) \leq \pm 0.5\%$  for commercial sampling.

- $s(FSE) \leq \pm 5.0\%$  for technical sampling and process control.

- $s(FSE) \leq \pm 16.0\%$  for environmental and exploratory sampling.

### 3.3 Comparison between sampling protocols using Pierre Gy's factors and HT

Table 3 shows the values of Pierre Gy's factors (Pitard, 1993) for gibbsite bauxite described in Equation (1). The mineralogical factor (c) consists of two components, the densities of the mineral of interest and gangue, and the lot grade. In this case, the factor *c* was admitted as being a standard value as shown in Table 3, since all alumina refineries in Brazil use gibbsite bauxite (Bortoleto *et al.*, 2019).

Table 3 - Gy's factors for gibbsite bauxite.

Factor	<i>c</i>	<i>f</i>	<i>g</i>	<i>d<sub>i</sub></i>	<i>IH<sub>L</sub></i>
Value	3.6	0.5	0.25	0.00036	0.0085 d <sup>2.5</sup>

As part of the last step of this study, the relative standard deviation of the fundamental sampling error *s(FSE)* was estimated using the Pierre Gy's factors as well as the parameters of *K* and  $\alpha$  obtained experimentally by the HT. The standard deviation was calculated for each step of the sampling and sample preparation protocol for each of the three deposits as shown in Table 4.

Table 4 - The sampling protocol and the relative standard deviation of the *s(FSE)* of each stage using Pierre Gy's factors as well as the results of HT.

Step	<i>M<sub>L</sub></i> (g)	<i>M<sub>s</sub></i> (g)	<i>d<sub>N</sub></i> (cm)	<i>s(FSE)</i> GY	<i>s(FSE)</i> HT		
					Deposit 1	Deposit 2	Deposit 3
Primary Sampling	1.500E+10	15000	5	0.563%	0.973%	0.426%	0.495%
Crushing	15000	15000	2.54	-	-	-	-
Primary Quartering	15000	2500	2.54	0.540%	1.051%	0.461%	0.579%
Grinding	2500	2500	0.2	-	-	-	-
Secondary Quartering	2500	200	0.2	0.084%	0.254%	0.112%	0.189%
Pulverization	200	200	0.015	-	-	-	-
<b>TOTAL</b>				<b>0.784%</b>	<b>1.455%</b>	<b>0.638%</b>	<b>0.784%</b>

Considering Equation (7), a maximum relative standard deviation of the fundamental sampling error *s(FSE)* of 5.0% and a high value for the initial lot mass (*M<sub>L</sub>*), the minimum sample mass (*M<sub>s</sub>*) to represent the primary sample at the mine, where *d<sub>N</sub>* is 5 cm, was calculated and is presented in Table 5.

Table 5 - Minimum sample masses (*M<sub>s</sub>*) for the primary sample at the mine.

Parameter	GY	HT		
		Deposit 1	Deposit 2	Deposit 3
<i>d<sub>N</sub></i> (cm)	5	5	5	5
<i>M<sub>s</sub></i> (g)	190	568	109	145

### 4. Conclusion

This article presents two different methods to estimate the relative standard deviation of the *s(FSE)* by applying the Pierre Gy's formula and using the results of the HT. HT allows obtaining the sampling parameters *K* and  $\alpha$ , which were compared with Gy's estimated parameters of the gibbsite bauxite.

Through the theory of sampling (TOS), it was possible to determine the estimated constitutional heterogeneity constant factor (*EST IH<sub>L</sub>*) present in each step of a sampling protocol and find the associated errors. An appropriate sampling protocol for any type of ore ensures the reliability of the process.

The evaluation of sampling bias should be done by incorporating all the principles discussed here to guarantee that the sampling process is equi-probabilistic. When dealing with sampling variability, the *s(FSE)* in each step of the sampling protocol should be observed to diagnose the critical sampling stages and act proactively to minimise the total error, and moreover, it is important to determine what is the minimum *M<sub>s</sub>* to represent all size fractions.

In Table 2, the comparison between *K* and  $\alpha$  parameters allow to conclude that there is a greater heterogeneity associated with the deposit 1. In the bauxite from deposits 2 and 3, the *K* and  $\alpha$  parameters

obtained experimentally were close to the estimated parameters using Gy's factors: *K*=0.0085 and  $\alpha$ =2.5, resulting in identical total values of Gy's *s(FSE)* and HT *s(FSE)* for the bauxite from Poços de Caldas.

The primary quartering step of the sampling protocol from deposit 1 showed greater contrast because of intrinsic heterogeneity. Therefore, it is possibly incorrect to assume the mineralogical factor (*c*) as a standard value for gibbsite bauxite in Gy's formula, as shown in Table 3.

Thus, it can be concluded that the biggest influence on the physical and chemical characteristics of the bauxite is the impact of the weathering process.

Fundamentally, the climatic factor and the exposure time in which the parent rock was subjected to adverse conditions of temperature and pressure can alter the shape, granulometric, mineralogical, and liberation factors, diversifying bauxites in

Brazil and worldwide.

Optimizing sampling protocols is not a simple task. The theory of sampling proposed by Pierre Gy suggests that additional experiments are necessary to complement the ones pro-

posed in international standards and to increase the reliability of the sample results, although the Gy's formula proved to be very effective in optimizing bauxite sampling protocols, mainly for deposits 2 and 3.

## Acknowledgements

The authors kindly express their sincere gratitude to the Department of

Mining and Petroleum Engineering and the University of São Paulo for their support.

## References

- ALVES, F. E. M.; SOUZA, B. A.; BORTOLETO, D. A.; HAJJ, T. M. Reconciliation of sampling data and heterogeneity analysis of a bauxite mine in Poços de Caldas, MG, Brazil. *REM - International Engineering Journal*, v. 73, n. 4, oct./dec. 2020.
- ARENARE, D. de S. *Caracterização de amostras de bauxita visando a aplicação de métodos de concentração gravítica*. 2008. Dissertação (Mestrado em Engenharia). Universidade Federal de Minas Gerais, 2009.
- ARIOLI, E. E.; ANDRIOTTI, J. L. S. *Representatividade da amostragem na prospecção geoquímica*. Companhia de Pesquisa de Recursos Minerais - CPRM. Produção científica, 2007.
- BORTOLETO, D. A.; CHIEREGATI, A. C.; PEREIRA, A. H. R.; OLIVEIRA, R. C. The application of sampling theory in bauxite protocols. *REM - Revista Escola de Minas*, v. 67, n. 2, p. 215-220, 2014.
- BORTOLETO, D. A.; CHIEREGATI, A.; OLIVEIRA, R. C. Optimizing the sampling protocols for aluminum ores-a new approach. *Mineralogy and Petrology*, v. 113, n. 4, p. 463-475, 2019.
- CARVALHO, A. *As bauxitas no Brasil: síntese de um programa de pesquisa*. Livre Docência, Instituto de Geociências - Universidade de São Paulo, 1989. 130 p.
- CHIEREGATI, A. C.; PITARD, F. F. *Tratamento de minérios*. 6. ed. Centro de Tecnologia Mineral - CETEM, 2018, cap. 2.
- ELLERT, R. Contribuição à geologia do maciço alcalino de Poços de Caldas. Faculdade de Filosofia, Ciências e Letras - Universidade de São Paulo, *Boletim Geologia*, v. 237, n. 18, p. 5-63, 1959.
- GY, P. M. *Sampling of particulate materials: theory and practice*. Elsevier Scientific Publishing Company, 2. ed. rev. 1982.
- GY, P. M. *Sampling for analytical purposes West Sussex*, England: JohnWiley & Sons, 1998. Traduzido por A.G. Royle.
- KOYAMA, I. K.; CHIEREGATI, A. C.; ESTON, S. M. Teste de heterogeneidade como método de otimização de protocolos de amostragem. *Brasil Mineral*, v. 27, p. 63-68, 2010.
- KOTTEK, M.; GRIESER, J.; BECK, C.; RUDOLF, B.; RUBEL, F. World map of the Köppen-Geiger climate classification updated. *Meteorologische Zeitschrift*, v. 15, n. 3, 259-263, 2006.
- LEONARDI, F. A.; LADEIRA, F. S. B.; SANTOS, M. Perfis bauxíticos do planalto de Poços de Caldas SP/MG: análise geoquímica e posição na paisagem. *Revista de Geografia*, n. 1, p. 45-48, 2010. Edição especial. SINAGEO, 8.
- LUZ, A. B.; SAMPAIO, J.; ALMEIDA, S. L. M. *Tratamento de minérios*. Centro de Tecnologia Mineral - CETEM. 4. ed, 2004.
- MINNITT, R. C. A.; RICE, P. M.; SPANGENBERG, C. Experimental calibration of sampling parameters K and alpha for Gy's formula by the sampling tree method. *The Journal of The Southern African Institute of Mining and Metallurgy*, p. 513-518, 2007, parte 2.
- MINNITT, R. C. A.; ASSIBEY-BONSU, W. A comparison between the duplicate series analysis method and the heterogeneity test as methods for calculating the sampling constants, K and alpha. *The Journal of The Southern African Institute of Mining and Metallurgy*, v. 110, p. 251-267, 2010.
- MONTEIRO, C. C.; SILVA, J. P. A. *Sumário mineral brasileiro*. Agência Nacional de Mineração - ANM, 2018.
- OLIVEIRA, F. S. *A bauxita de Barro Alto (GO): gênese e evolução mineralógica, micromorfológica e geoquímica*. 2011. Dissertação (Mestrado em Evolução Crustal e Recursos Naturais) - Departamento de Geologia - Escola de Minas - Universidade Federal de Ouro Preto, 2011, 149 f.
- PATTERSON, S. H. Bauxite reserves and potential aluminum resources of the world. *U.S. Geol. Surv. Bull.* Washington, DC, 1967.
- PITARD, F. F. *Pierre Gy's sampling theory and sampling practice*. 2. ed, Boca Raton, 1993.
- PITARD, F. F. Effects of residual variances on the estimation of variance of the fundamental error. *Chemometrics and Intelligent Laboratory Systems*, 2004.
- PITARD, F. F. Sampling correctness: a comprehensive guide. WORLD CONFERENCE ON SAMPLING AND BLENDING, 2, p. 55-68, 2005.
- SAMPAIO, J. A.; ANDRADE, M. C.; DUTRA, A. J. B. Bauxita. In: LUZ, A. B.; LINS, F. A. F. (ed) *Rochas e minerais*

- industriais*: usos e especificações, 2. ed. Rio de Janeiro: CETEM/MCT, 2008. p. 311-337. cap. 14.
- SANTOS, W. M. *Mineralogia e geoquímica da bauxita derivada do anortosito, Barro Alto, Goiás*. Dissertação (Mestrado) - Instituto de Geociências - Universidade de Brasília, 2011.
- SILVA, B. A. *Aplicação do teste de heterogeneidade tradicional na bauxita de Poços de Caldas, MG*. 2019. Trabalho de Conclusão de Curso (Graduação) - Departamento de Engenharia de Minas - Universidade Federal de Alfenas, 2019. 35 f.

---

Received: 1 June 2022 - Accepted: 21 February 2023.



All content of the journal, except where identified, is licensed under a Creative Commons attribution-type BY.